Deep-level transient spectroscopy studies of defects in GaAs-AlGaAs superlattices

P. A. Martin,[a] K. Hess, M. Emanuel, and J. J. Coleman
Coordinated Science Laboratory, Department of Electrical and Computer Engineering, University of Illinois, Urbana, Illinois 61801

(Received 18 April 1986; accepted for publication 23 June 1986)

We present preliminary results of a study of defects in GaAs-AlGaAs superlattices using deep-level transient spectroscopy (DLTS). A dramatic difference is observed between the DLTS spectra of two superlattices when the superlattice period is doubled. This is explained by the presence of miniband conduction in the case of the smaller period and its absence in the case of the larger, and by the consequent difference in the distribution of electrons in the superlattice. Observed activation energies must be reinterpreted for comparisons to bulk material.

Ever since the original proposal of superlattice structures by Esaki and Tsu[1] the prospect of engineering the band structure of new semiconductor materials has inspired a great deal of work in the field. Superlattices have been proposed as substrates for integrated optoelectronics[2] and for a variety of novel photodiode structures.[3] Studies of defects in these structures have shown that, with suitable doping profiles, it is possible to reduce substantially the troublesome persistent photoconductivity effect associated with the *DX* center in the AlGaAs alloy.[4,5] (The *DX* center is so named after Lang and Logan's original model of a donor *D* paired to an unknown defect *X*.[6]) Due to the importance of defects in controlling electronic properties of materials and in limiting the performance of devices, there is a need for studies of electronic defects in these structures. We present here deep-level transient spectroscopy (DLTS)[7] studies of defects in GaAs-AlGaAs superlattices which suggest that activation energies measured in such structures must be interpreted with care with regard to the method of conduction in the structure.

The samples studied in the present work were grown by metalorganic chemical vapor deposition. The sample consists of a GaAs buffer layer grown on top of a conducting GaAs substrate, followed by a superlattice consisting of alternating layers of GaAs and $Al_xGa_{1-x}As$ ($x = 0.5$). Two wafers were grown, one with 100-Å layers of each material and one with 50-Å layers. A total superlattice thickness of 2 μm was used in each case to avoid depleting into the substrate in the course of the experiment. Both superlattices were doped uniformly to 9×10^{16} cm^{-3}. Growth parameters were identical for the two samples with the sole exception of the layer thicknesses.

For diode fabrication, ohmic contacts were formed on the backside by evaporation of Au-Ge-Ni contacts and alloying. After an HCl etch to remove any oxide, Au was evaporated on the epitaxial side to form Schottky barriers defined by photolithographic lift-off in a pattern of 8-mil dots. 12-mil mesas were etched using a 5:1:1 solution of H_2SO_4:H_2O:H_2O_2 and diodes were cleaved and attached with silver-filled epoxy to TO-18 headers. Contact was made to the Schottky barrier using thermocompression wire bonding. The diodes show a forward turn-on voltage of about 0.5 V and a reverse breakdown voltage of 6–8 V. *C-V* profiling confirmed the doping level, but did not show any periodic variation of the carrier concentration for either superlattice. The room-temperature Debye length is about 140 Å, which is too large to permit resolution of the nonuniform carrier concentration in even the 100 Å superlattice.

Deep-level transient spectroscopy (DLTS) was performed using a system described elsewhere.[8] Results for the two samples described above are shown in Fig. 1. All of the DLTS peaks shifted to lower temperatures as the reverse bias was increased, indicating the presence of electric field effects.[6] Thus, data cited were obtained with a quiescent reverse bias of 1 V in order to minimize these effects. From integration of the *C-V* profile, we calculate an electric field in these diodes of about 6.6×10^4 V/cm at this bias level. The 50-Å superlattice shows three defect levels labeled A, B, and C. The 100-Å superlattice shows only one defect level, D, which does not correspond to any of the levels observed in the 50-Å layers. Activation energies (E_i), capture cross sections (σ), and defect concentrations (N_{TT}) are summarized in Table I. Capture cross sections were obtained from the Arrhenius plot. Defect concentrations include a correction for the edge effect[9] and are calculated assuming the observed

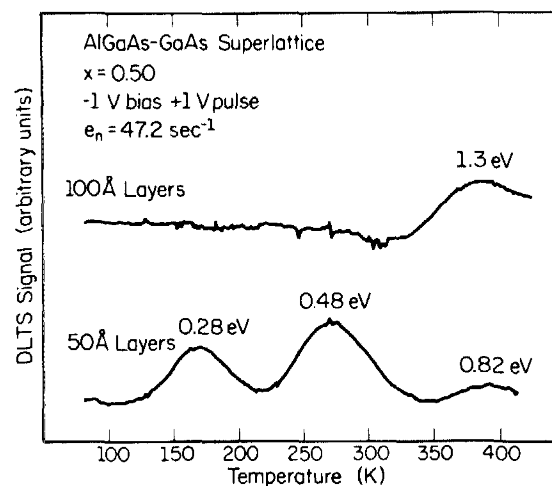

FIG. 1. DLTS spectra of 100- and 50-Å layer samples.

[a] Present address: General Electric Electronics Laboratory, Syracuse, New York 13221.

 0021-8979/86/202882-04$02.40 © 1986 American Institute of Physics

TABLE I. Defect levels observed in two superlattices. Levels A, B, and C occur only in the superlattice with 50-Å layers, while level D occurs only in the superlattice with 100-Å layers.

Defect level	E_t (eV)	σ (10^{-15} cm^2)	N_{TT} (10^{14} cm^{-3})
A	0.28 ± 0.02	1.2	18.0
B	0.48 ± 0.02	1.4	27.0
C	0.82 ± 0.03	42.0	8.8
D	1.30 ± 0.13	9.3×10^8	54.0

uniform concentrations. In the event that a defect is characteristic of only one of the layers (e.g., GaAs but not AlGaAs) the defect concentrations in those layers would be twice the value listed in Table I.

We do not expect dramatic variations in defect spectra from variations in crystal quality between consecutive growth runs in the same system, and we have not observed such variations in previous studies. The only difference between the two samples is, thus, in the layer thicknesses. In the case of the 100-Å superlattice, we do not expect miniband conduction normal to the layers. In the case of the 50-Å layer sample, however, the lowest miniband is considerably wider, and miniband conduction is plausible. If this is the case, the DLTS experiment will sweep detrapped carriers out of the space-charge region by way of the superlattice miniband in the case of the thinner layers, and the observed activation energies will be with respect to the miniband, rather than with respect to the bulk conduction band edges of either the GaAs or the AlGaAs. In the case of thicker layers, however, carriers emitted from defect levels must surmount the AlGaAs barriers (or undergo tunneling with rather long time constants) before they can be swept out of the space-charge region and produce the observed capacitance transients. The two cases are illustrated in Fig. 2. E_{50} and E_{100} are the lowest miniband energies for the 50- and 100-Å superlattice, respectively.

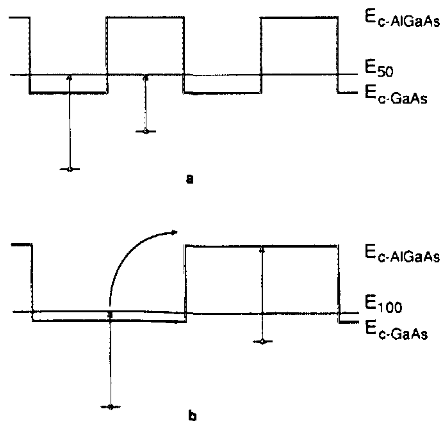

FIG. 2. Ionization of defect levels in the presence and absence of miniband conduction. (a) With a conducting miniband, trapped carriers emit to the miniband level E_{50} and are swept out of the junction through the miniband. (b) In the case of a nonconducting miniband E_{100} carriers must surmount the AlGaAs barriers before they can be swept out of the space-charge region.

This raises the question of how defects and defect activation energies measured in bulk material will correspond to those observed in the superlattice. Unlike shallow donor levels, deep levels are determined by a central cell potential which leaves the trapped electron tightly bound in real space.[10] For the layer thicknesses studied here, an electron tightly bound by a central cell potential will "see" only the layer in which it is located, either GaAs or AlGaAs. We expect, therefore, that defects will remain at the same energy with respect to the bulk band edges as observed in bulk material, but that the activation energies measured in a DLTS experiment may differ from the bulk activation energies depending on the layer in which the defect resides and the band into which it emits. In the limit of much thinner layers, deep-level wave functions and activation energies will be determined by the band structure of the superlattice and may not relate to observations in bulk material. It is not yet clear at what layer thickness this transition will occur, but we expect it to be much less than 50 Å.

This picture forces a reinterpretation of our activation energies, as shown in Fig. 3. The shaded bands represent the defect energies with respect to the miniband level E_{50} in the case of the 50-Å superlattice [Fig. 3(a)] and with respect to the AlGaAs band edge in the case of the 100-Å superlattice [Fig. 3(b)]. The vertical height of the shaded bands represents the experimental uncertainty of the activation energy in each case, as listed in Table I. We can make some tentative assignments for which of the layers (GaAs or AlGaAs or both) serves as the host of each of these defects by comparing

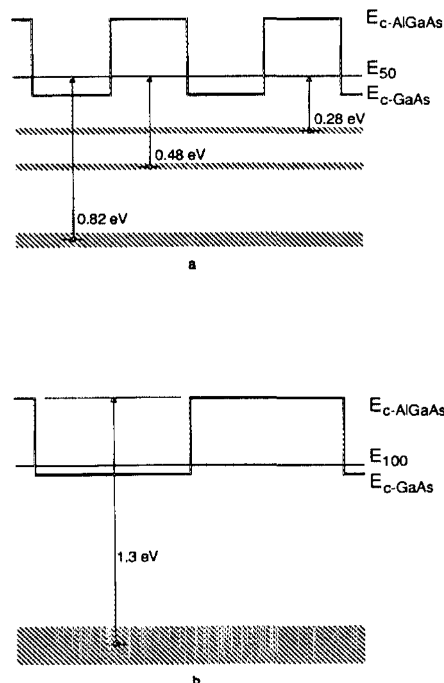

FIG. 3. Reinterpretation of observed activation energies. (a) In the presence of a conducting miniband the observed activation energies are with respect to the miniband level for the 50-Å superlattice E_{50}. (b) In the absence of conduction through the miniband at E_{100}, observed activation energies are with respect to the AlGaAs conduction-band edge. The vertical height of the shaded bars reflect the experimental uncertainty of the measured activation energies.

TABLE II. Tentative defect assignments, including the layer of the superlattice in which each defect is believed to reside, and the band to which emission of electrons is observed.

Defect level	E_i^{bulk} (eV)	Corresponds to	In layer	Emitting to
A	0.58 ± 0.02	see text	AlGaAs	E_{50}
B	0.78 ± 0.02	EL2	AlGaAs	E_{50}
C	0.72 ± 0.03	EL2	GaAs	E_{50}
D	0.89 ± 0.13	EL2	GaAs	$E_{c\text{-AlGaAs}}$

a recomputed activation energy with respect to bulk band edges with defect activation energies observed in bulk MOCVD GaAs and AlGaAs. To calculate an activation energy with respect to the bulk band edge E_c^{bulk}, we need values for ΔE_c, E_{50}, and E_{100}. We calculate the two miniband energies by a Kronig–Penney model, which gives us $E_{50} = 0.10$ eV and $E_{100} = 0.039$ eV. The choice of a value for the conduction-band discontinuity ΔE_c is more problematic. We have chosen the results of Wolford *et al.* who have performed optical measurements under pressure which are likely to be much more accurate and direct than many competing techniques.[11] This work cites $\Delta E_c \approx 0.7 \Delta E_g$ corresponding to 0.406 eV for these samples. A set of tentative identifications of each of these levels is shown in Table II.

If level D observed in the 100-Å layers is assumed to be activated with respect to the top of the AlGaAs barriers, within the accuracy of these data it lines up well with the EL2 level in GaAs.[12] We take the results of Gatos and Lagowski[13] as the most accurate measurements of activation energy and capture cross section of EL2: 0.814 eV and 2.6×10^{-13} cm^2, respectively. The anomalously high capture cross section which we observe for our level D is explained by the highly nonuniform distribution of carriers, which lie predominantly in the GaAs layers. In analogy to the case of free carrier tails in an ordinary diode,[14] this nonuniformity can result in a nonexponential transient, distorting both the capture cross section and the activation energy observed for this level. The distorted peak shape for level D is consistent with a nonexponential transient. If, for example, one assumes the true value of the capture cross section for level D is the same as for level C, one obtains a corrected value of 0.74 eV for the activation energy of level D. If one further assumes activation with respect to the 100-Å miniband, this results in a bulk activation energy E_i^{bulk} of 0.70 eV in the GaAs layers, a result very similar to level C. This is still within experimental error of the EL2 level in GaAs, so the only uncertainty is in the nature of the emission process. Emission to the miniband does not necessarily imply miniband conduction, as the initial transition could be followed by very rapid emission to the AlGaAs band edge. Analysis of nonexponential transients requires a more sophisticated analysis than that presented here, so these numerical corrections are approximate and tentative. In accordance with this, we have omitted the corrections for nonexponentiality in the accompanying figures and tables. The importance of the nonexponential transients, however, is clear. The effect is either less pronounced or completely absent in the 50-Å superlattice, where the carrier concentration is more uniform. In accordance with the nonuniform carrier concentration in the 100-Å superlattice, there are few carriers in the AlGaAs layers available for capture by AlGaAs traps. This explains the absence of a corresponding peak for EL2 in the AlGaAs. Level D shows a much stronger field effect than expected for the high temperatures at which it is observed and higher than observed for EL2 in GaAs.[15,16] This is explained by the presence of electric fields caused by the superlattice itself.

If we assume that activation energies observed in the 50-Å superlattice are with respect to the 50-Å miniband, the DLTS results for that superlattice are explained quite well. Level B lines up well with the EL2 level in AlGaAs emitting to the superlattice miniband. EL2 has been consistently observed as a dominant level in $Al_xGa_{1-x}As$ for $0 \leqslant x \leqslant 0.5$ with an activation energy which remains unchanged as the alloy composition is varied and a capture cross section which decreases with x.[17] Miniband conduction leads to a higher electron concentration in the AlGaAs and makes observation of AlGaAs defects possible, but this is still only a matter of degree. Electron concentration is still nonuniform, and the observed concentration of level B is probably lower than the actual EL2 concentration in the AlGaAs layers. Level C could be assigned either to EL2 in the AlGaAs emitting to the AlGaAs band edge or to EL2 in the GaAs emitting to the miniband. The latter is more likely, however, since, if miniband conduction is possible it provides a smaller activation energy and higher emission rate which would dominate emission to the higher AlGaAs conduction-band edge. This leaves a poor lineup between level C and EL2 in the GaAs which can probably be accounted for by field effects, errors in the use of the Kronig–Penney model to calculate miniband levels for thin layers ($L_z \leqslant 100$ Å), and variations in the precise values of layer thicknesses used to calculate the miniband levels. Level A could lie in either layer. E_i^{bulk} corresponds to 0.17 eV in the case of a GaAs trap or 0.58 eV in the case of an AlGaAs trap. This level shows a very steep field dependence, which is expected since field effects are much stronger at low temperatures. At the low temperatures at which level A is observed the electric field is more than enough to give an apparent activation energy which is below the true value.[18] It is possible that this level's absence in the 100-Å superlattice is due to the presence of higher fields raising the emission rate beyond that which the system can detect. The system used in this work was not equipped for temperatures lower than 77 K, so it was not possible to investigate this possibility. Assignment to an AlGaAs level would provide a more convincing explanation of the center's absence in the 100-Å superlattice due to the difficulty of capturing electrons into AlGaAs defects. The most likely assignment is to a defect with a larger activation energy such as the 0.25 ± 0.02 eV trap observed by Bhattacharya *et al.*[19,20] in GaAs, or, the 0.62-eV level observed by many workers in AlGaAs.[19,20] We feel the AlGaAs level is more likely, since defect concentrations are known to be much higher in AlGaAs than in GaAs, and because its absence in the 100-Å superlattice is more easily explained without any assumption

about field dependence in that superlattice.

In summary, we have presented the results of a study of defects in GaAs–AlGaAs superlattices which suggest that activation energies observed from defects in these structures must be interpreted with care with regard to the method of conduction in the structure in question. These data are consistent with a picture of deep levels bound by central cell potentials which remain unperturbed by layer thicknesses as small as 50 Å. In analogy to defect studies in semiconductor alloys, superlattices present a potential tool for studying the physics of defect states by varying the host lattice.

This work was supported by the Office of Naval Research under contract number N00014-76-C-0806 and by the Army Research Office under contract number DAAG29-85-K-0133.

[1]L. Esaki and R. Tsu, IBM J. Res. Dev. **14**, 61 (1970).

[2]N. Holonyak, Jr., W. D. Ladig, M. D. Camras, J. J. Coleman, and P. D. Dapkus, Appl. Phys. Lett. **39**, 102 (1981).

[3]Federico Capasso, Surf. Sci. **132**, 527 (1983).

[4]Toshio Baba, Takashi Mizutani, and Masaki Ogawa, Jpn. J. Appl. Phys. **22**, L627 (1983).

[5]Toshio Baba, Takashi Mizutani, and Masaki Ogawa, J. Appl. Phys. **59**, 526 (1986).

[6]D. V. Lang and R. A. Logan, Phys. Rev. B **19**, 1015 (1979).

[7]D. V. Lang, J. Appl. Phys. **45**, 3023 (1974).

[8]D. S. Day, M. J. Helix, K. Hess, and B. G. Streetman, Rev. Sci. Instrum. **50**, 1571 (1979).

[9]D. V. Lang, in *Thermally Stimulated Relaxation in Solids*, edited by P. Braunlich (Springer, Berlin, 1978), pp. 93–133.

[10]Harold P. Hjalmarson, P. Vogl, D. J. Wolford, and John D. Dow, Phys. Rev. Lett. **44**, 810 (1980).

[11]D. J. Wolford, T. F. Kuech, J. A. Bradley, M. A. Gell, D. Ninuo, and M. Jaros, presented at the Thirteenth Annual Conference on the Physics and Chemistry of Semiconductor Interfaces, Pasadena, CA, January 1986 (unpublished).

[12]G. M. Martin, A. Mitonneau, and A. Mircea, Electron. Lett. **13**, 191 (1977).

[13]H. C. Gatos and J. Lagowski, Mater. Res. Symp. Proc. **46**, 153 (1985).

[14]J. M. Noras, Solid State Commun. **39**, 1225 (1981).

[15]G. Vincent, A. Chantre, and D. Bois, J. Appl. Phys. **50**, 5484 (1979).

[16]S. Makram-Ebied, in *Materials Research Society Symposium Proceedings*, edited by J. Narayan and T. Y. Tan (North-Holland, New York, 1980), Vol. 2, p. 495.

[17]T. Matsumoto, P. K. Bhattacharya, J. Darmawan, and M. J. Ludowise, Inst. Phys. Conf. Ser. **65**, 289 (1983).

[18]P. A. Martin, B. G. Streetman, and K. Hess, J. Appl. Phys. **52**, 7409 (1981).

[19]P. K. Bhattacharya, S. Subramanian, and M. J. Ludowise, J. Appl. Phys. **55**, 3664 (1984).

[20]P. K. Bhattacharya, T. Matsumoto, and S. Subramanian, J. Cryst. Growth **68**, 301 (1984).

Journal of Applied Physics is copyrighted by the American Institute of Physics (AIP). Redistribution of journal material is subject to the AIP online journal license and/or AIP copyright. For more information, see http://ojps.aip.org/japo/japcr/jsp
Copyright of Journal of Applied Physics is the property of American Institute of Physics and its content may not be copied or emailed to multiple sites or posted to a listserv without the copyright holder's express written permission. However, users may print, download, or email articles for individual use.